PHYSICAL REVIEW A **76**, 041602(R) (2007)

Magnetic and superfluid phases of confined fermions in two-dimensional optical lattices

Brian M. Andersen and G. M. Bruun
Niels Bohr Institute, University of Copenhagen, Universitetsparken 5, DK-2100 Copenhagen Ø, Denmark
(Received 25 June 2007; published 19 October 2007)

We examine antiferromagnetic and *d*-wave superfluid phases of cold fermionic atoms with repulsive interactions in a two-dimensional optical lattice combined with a harmonic trapping potential. For experimentally realistic parameters, the trapping potential leads to the coexistence of magnetic and superfluid ordered phases with the normal phase. We study the intriguing shell structures arising from the competition between the magnetic and superfluid order as a function of the filling fraction. In certain cases, antiferromagnetism induces superfluidity by charge redistributions. We furthermore demonstrate how these shell structures can be detected as distinct antibunching dips and pairing peaks in the density-density correlation function probed in expansion experiments.

DOI: 10.1103/PhysRevA.76.041602 PACS number(s): 03.75.Ss, 05.30.Fk, 74.25.Ha, 74.72.−h

The trapping of ultracold atoms in optical lattices opens up the possibility to study quantum systems in periodic potentials with unprecedented experimental versatility. One can mimic strongly correlated systems relevant for paradigmatic condensed matter applications, as well as creating entirely new structures. The pace of experimental progress is impressive. The quantum phase transition between a superfluid and a Mott insulator has been observed for bosons [1], and Fermi surface effects were reported for fermions [2]. Bunching and antibunching effects in the density-density correlations were found for bosons and fermions in expansion experiments [3] and evidence of *s*-wave pairing was recently presented [4].

A major goal is to study two-component ($\sigma=\pm$) fermionic atoms in a two-dimensional (2D) optical lattice with repulsive interactions. Such a system is well described by the Hubbard model whose phase diagram is controversial and directly related to the physics of high-T_c superconductors. For filling fractions close to one particle per site ($n=1$), the system is antiferromagnetic (AF), whereas for smaller densities the true ground state is unknown. An important question is whether a *d*-wave superconducting state arises solely from repulsive interactions, but many other open questions remain, including suggested stripe and checkerboard charge-ordered ground states [5] that possibly coexist with superconductivity for some range of doping $x=1-n$. Experimentally, there is strong evidence for such inhomogeneous states in the cuprates [5–7], but it is unclear if they are important for pairing. An aim of the cold gas experiments is to improve our understanding of this complicated problem.

Motivated by this, we study a two-component gas of fermionic atoms in a 2D optical lattice. We include an external harmonic potential which originates from the Gaussian profile of the laser beams generating the trap. A main purpose of this paper is to study the interplay between this harmonic trapping potential and two of the most dominating ordered phases of the homogeneous Hubbard model: the antiferromagnetic and *d*-wave superconducting phases. Previous theoretical studies have focused on the one-dimensional case [8]. For realistic parameters, we find that the magnetic and *d*-wave superfluid (DSF) phases coexist and form shell structures, in analogy with what has been observed for bosons [9]. We then examine how these shell structures can be detected in density-density correlations by expansion experiments similar to those performed for ideal gases [3].

A two-component Fermi gas in an optical lattice is well described by the Hubbard model [10,11]

$$\hat{H}=-t\sum_{\langle ij\rangle,\sigma}\hat{a}^\dagger_{i\sigma}\hat{a}_{j\sigma}-\mu\sum_{i\sigma}\hat{n}_{i\sigma}+U\sum_i\hat{n}_{i\uparrow}\hat{n}_{i\downarrow}+\frac{1}{2}m\omega^2\sum_{i\sigma}R_i^2\hat{n}_{i\sigma}, \tag{1}$$

where $\hat{a}_{i\sigma}$ are annihilation operators for localized atoms on site i [at position $\mathbf{R}_i=(X_i,Y_i)$] with spin σ and $\hat{n}_{i\sigma}=\hat{a}^\dagger_{i\sigma}\hat{a}_{i\sigma}$ is the number operator. The parameters t and $U>0$ denote hopping between nearest-neighbor sites $\langle ij\rangle$ and on-site repulsion, respectively. They can be obtained from the atom-atom scattering length and the lowest-band Wannier state [12]. The last term in Eq. (1) describes the harmonic trapping potential. We use the unrestricted Hartree-Fock approximation to decouple the interaction term in Eq. (1).

In addition to the AF state at half filling, numerical methods indicate that the repulsive Hubbard model prefers *d*-wave superconducting order in a certain region of the U-x phase diagram [13]. Therefore, in a harmonic trap we expect that AF and superfluid order may coexist in the atomic cloud. To model this we include explicitly a BCS *d*-wave term so that the final mean-field Hamiltonian becomes

$$\hat{H}=-t\sum_{\langle ij\rangle,\sigma}\hat{a}^\dagger_{i\sigma}\hat{a}_{j\sigma}-\mu\sum_{i\sigma}\hat{n}_{i\sigma}+\frac{1}{2}m\omega^2\sum_{i\sigma}R_i^2\hat{n}_{i\sigma} + U\sum_i[\langle\hat{n}_{i\uparrow}\rangle\hat{n}_{i\downarrow}+\hat{n}_{i\uparrow}\langle\hat{n}_{i\downarrow}\rangle]+\sum_{\langle ij\rangle}[\Delta_{ij}a^\dagger_{i\uparrow}a^\dagger_{j\downarrow}+\text{H.c.}]. \tag{2}$$

It is well known that a nearest-neighbor attraction can generate such a *d*-wave BCS term at the self-consistent level [14]. We stress that even though our mean-field model Eq. (2) is phenomenological, it captures the existence and competition of ordered phases at $T=0$ such as AF and superfluidity, and has been widely used previously in the high-T_c community [14]. Note that even in 1D it is possible to obtain qualitative information from mean-field theory, such as, e.g., the shape of the density profiles and the existence of antiferromagnetic correlations [8]. This gives further confidence in the 2D $T=0$ mean-field results presented below.

Equation (2) can be diagonalized by the transformation $\hat{a}_{i\sigma}^{\dagger}=\Sigma_{E_{n\sigma}>0}[u_{n\sigma}^{*}(i)\hat{\gamma}_{n\sigma}^{\dagger}+\sigma v_{n\sigma}(i)\hat{\gamma}_{n-\sigma}]$ yielding the Bogoliubov–de Gennes equations

$$\sum_{j}\begin{pmatrix}\mathcal{K}_{ij}^{+} & \mathcal{D}_{ij}\\ \mathcal{D}_{ij}^{*} & -\mathcal{K}_{ij}^{-}\end{pmatrix}\begin{pmatrix}u_{n\sigma}(j)\\ v_{n-\sigma}(j)\end{pmatrix}=E_{n\sigma}\begin{pmatrix}u_{n\sigma}(i)\\ v_{n-\sigma}(i)\end{pmatrix}. \quad (3)$$

The diagonal blocks are given by $\mathcal{K}_{ij}^{\pm}=-t\delta_{\langle ij\rangle}+(V_i-\mu+U\langle\hat{n}_{i\mp\sigma}\rangle)\delta_{ij}$, where $V_i=\frac{1}{2}m\omega^2R_i^2$, and δ_{ij} and $\delta_{\langle ij\rangle}$ are the Kronecker delta symbols connecting on-site and nearest-neighbor sites, respectively. The off-diagonal block is $\mathcal{D}_{ij}=\delta_{\langle ij\rangle}\Delta_{ij}$, where in the homogeneous case $\Delta_{ij}=+(-)\Delta$ on the x (y) links corresponding to bulk $d_{x^2-y^2}$-wave pairing symmetry. Below, we restrict the discussion to $T=0$ and enforce self-consistency through iteration of the relations $\langle\hat{n}_{i\sigma}\rangle=\Sigma_n|v_{n\sigma}(i)|^2$ and $\Delta_{ij}=V_d\langle\hat{a}_{i\uparrow}\hat{a}_{j\downarrow}-\hat{a}_{i\downarrow}\hat{a}_{j\uparrow}\rangle=V_d\Sigma_n[u_{n\uparrow}(i)v_{n\downarrow}^{*}(j)-u_{n\uparrow}(j)v_{n\downarrow}^{*}(i)]$. Here, V_d is a coupling constant which, in principle, is a function of U, but at the phenomenological level becomes an independent parameter.

We now present our results of the numerical solution of the mean-field equations varying the number of particles N trapped in a potential with $\frac{1}{2}m\omega^2d^2/t=0.025$ where $d=1$ is the lattice spacing. This yields experimentally realistic lattice sizes of the order $\sim 40\times 40$. For these relatively small systems and the parameters used in this paper, the superfluid coherence length ξ is comparable to the characteristic length scale λ of the ordered phases. Therefore, we include the trapping potential exactly since the local density approximation cannot be expected to be valid because it assumes that $\xi\ll\lambda$. We first discuss the situation with no DSF order, i.e., $V_d=0$, and use an $N\times N$ square lattice ($N=44$) with open boundary conditions. In Fig. 1 we plot the density profile $n_i=\langle\hat{n}_{i\uparrow}\rangle+\langle\hat{n}_{i\downarrow}\rangle$ and the staggered magnetization $m_i=(-1)^{X_i+Y_i}(\langle\hat{n}_{i\uparrow}\rangle-\langle\hat{n}_{i\downarrow}\rangle)/2$ with $U/t=4.0$ for a varying number of trapped particles. The dashed lines in the left column display the density profile for an ideal gas ($U=0$). For sufficiently high density (top panel), the center region is a band insulator in both the interacting and noninteracting limits. We see that the main effect of the interaction is the formation of AF regions at densities $n\simeq 1$. Since the system is inhomogeneous due to the trapping potential, the AF order coexists with the normal phase. This leads to steps in the density profile as the magnetic correlations favor $n\simeq 1$. At the same time, the density is reduced in the center of the trap and the atomic cloud becomes more extended. Upon reducing the number of particles in the trap, the magnetization is seen to evolve from a ring structure to a center island.

For larger systems, spin-density waves with ordering vectors other than the conventional AF $\mathbf{Q}=(\pi,\pi)$, e.g., stripe phases known from high-T_c materials, may become evident at filling away from $n\simeq 1$. In that case we expect the same overall results as those in Fig. 1 but with magnetism existing for a wider doping range.

Next we discuss the possibility of superfluid order, focusing on both the spatial distribution and the interplay with the magnetic order. In Fig. 2 we show the d-wave order param-

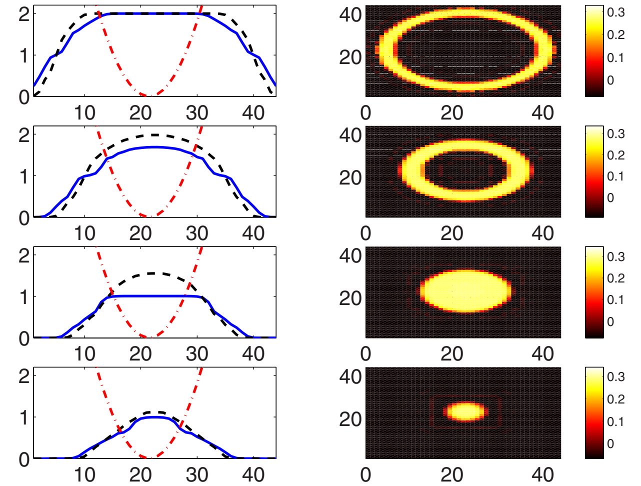

FIG. 1. (Color online) Left: line cut of the density (blue, solid lines) and trap potential (red, dot-dashed lines) through the center of the (spherically symmetric) trap, $U/t=4.0$. The black dashed lines show the density profile for the noninteracting case, $U=0$. Right: the associated real-space staggered magnetization. The total number of fermions in the 44×44 system is (top to bottom) 1936, 968, 484, 242.

eter (left) defined as $\Delta_i=(1/4)(\Delta_{i,i+\hat{x}}+\Delta_{i,i-\hat{x}}-\Delta_{i,i+\hat{y}}-\Delta_{i,i-\hat{y}})$, where $\hat{x}$ ($\hat{y}$) are the unit vectors along the x (y) axis, and the magnetization (right column). The density profiles (not shown) are similar to those presented in Fig. 1. The spatial structures depicted in Fig. 2 come from the interplay between the trapping potential and the magnetic and superfluid correlations and can be understood as follows. The amplitude of Δ peaks at one particle per site just like the AF order. This leads to a competition between DSF and AF order in regions around $n\simeq 1$. We have chosen $V_d/t=2.0$ giving $\Delta\sim 0.15t$ (and a coherence length of a few lattice spacings) consistent with the numerical results of Ref. [13]. For the resulting ratio $V_d/U=1/2$, antiferromagnetism dominates and DSF order is

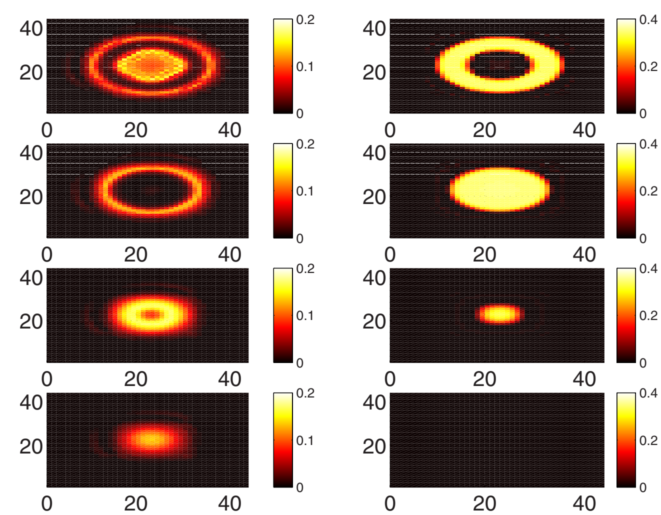

FIG. 2. (Color online) Left: spatial dependence of the d-wave superfluid order Δ_i with $V_d/t=2.0$ and $U/t=4.0$. Right: staggered magnetization obtained for the same set of parameters. The total number of fermions is (top to bottom) 726, 484, 242, 144.

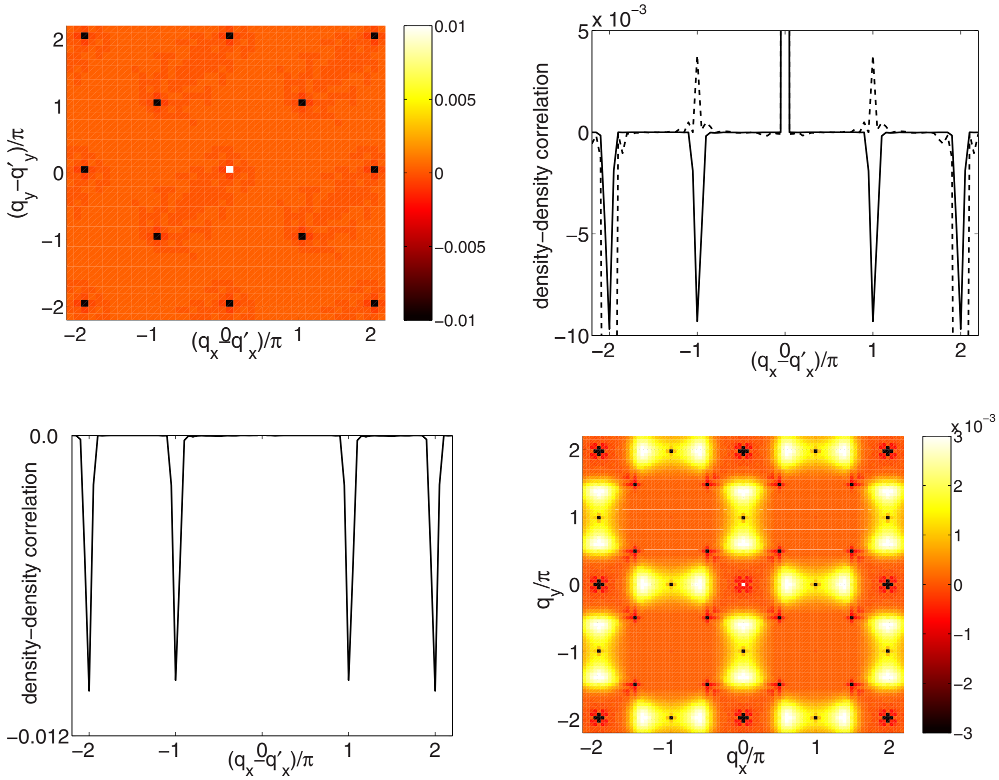

FIG. 3. (Color online) (Top row) Density-density correlation function $\mathcal{C}$ versus $\mathbf{q}-\mathbf{q}'$ (left) with $\mathbf{q}'=(\pi/2,\pi/2)$, and a cut (right) along the diagonal $q_x-q_x'=q_y-q_y'$. Parameters are identical to those used in Fig. 1 (third row). (Lower left) $\mathcal{C}(\mathbf{q},\mathbf{q}')$ along a diagonal with $q_x-q_x'=q_y-q_y'$ and $\mathbf{q}'=(\pi/2,\pi/2)$ (solid line) and along a horizontal cut q_x-q_x' with $q_y=0$ and $\mathbf{q}'=(\pi/2,0)$ (dashed line) for the same parameters as in Fig. 2 (second row). (Lower right) $\mathcal{C}(\mathbf{q},\mathbf{q}')$ versus $\mathbf{q}$ when $\mathbf{q}'=-\mathbf{q}$.

generally left to exist in regions surrounding the AF order. This is seen, for example, in the two middle rows of Fig. 2, where AF exists in a center island with $n\simeq 1$ surrounded by a ring of DSF. This is also the origin of the outer rim of the remarkable double-ring structure shown in the top left subplot of Fig. 2. There, however, the center DSF island is a case where magnetism surprisingly promotes DSF because of charge redistributions: The AF order decreases the density in the center of the trap below the threshold for generating DSF. For sufficiently small fillings, only a superfluid cloud is left in the trap (bottom row in Fig. 2).

We now address the important question of how the shell structures presented in Figs. 1 and 2 can be detected experimentally. Since magnetic and superfluid order coexist with the normal phase, it is *a priori* unclear how strong their experimental signatures will be. A well-known experimental technique is to measure the density-density correlations of an expanding gas after the lattice has been switched off. The density-density correlation function $\langle n(\mathbf{r})n(\mathbf{r}')\rangle$ after expansion time t probes the momentum correlation function $\langle n_{\mathbf{q}}n_{\mathbf{q}'}\rangle$ for the interacting system before the expansion with $n_{\mathbf{q}}=\Sigma_\sigma a^\dagger_{\mathbf{q}\sigma}a_{\mathbf{q}\sigma}$ and $\mathbf{r}=\mathbf{q}t/m$ [15]. We focus on the correlation function

$$\mathcal{C}(\mathbf{q},\mathbf{q}') = \langle n_{\mathbf{q}}n_{\mathbf{q}'}\rangle - \langle n_{\mathbf{q}}\rangle\langle n_{\mathbf{q}'}\rangle = \delta_{\mathbf{q},\mathbf{q}'}\langle n_{\mathbf{q}}\rangle - \left|\sum_{n\sigma} b^*_{\mathbf{q}'n\sigma}b_{\mathbf{q}n\sigma}\right|^2 + \sum_{nm\sigma} b^*_{\mathbf{q}'n\sigma}a^*_{\mathbf{q}n\sigma}a_{\mathbf{q}m\sigma}b_{\mathbf{q}'m\sigma}, \qquad (4)$$

where $a_{\mathbf{q}n\sigma}$ $(b_{\mathbf{q}n\sigma})=(1/N)\Sigma_i u_{in\sigma}(v_{in\sigma})\exp(-i\mathbf{q}\cdot\mathbf{R}_i)$. For noninteracting fermions, $\mathcal{C}(\mathbf{q},\mathbf{q}')$ has antibunching dips for $\mathbf{q}-\mathbf{q}'=(n_x2\pi,n_y2\pi)$ where n_x and n_y are integers as was recently observed [3]. Atoms forming an AF state will in addition exhibit antibunching dips in $\mathcal{C}(\mathbf{q},\mathbf{q}')$ for $\mathbf{q}-\mathbf{q}'=(n_x\pi,n_y\pi)$ with odd integers n_x,n_y, reflecting the period doubling due to the magnetic order. For a system without an external trapping potential characterized by an AF order parameter $m=|\langle n_{i\uparrow}\rangle-\langle n_{i\downarrow}\rangle|/2$, mean-field theory yields $\langle n_{\mathbf{q}}n_{\mathbf{q}'}\rangle=\langle n_{\mathbf{q}}\rangle\langle n_{\mathbf{q}'}\rangle-\Sigma_\sigma\langle a^\dagger_{\mathbf{q}\sigma}a_{\mathbf{q}'\sigma}\rangle\langle a^\dagger_{\mathbf{q}'\sigma}a_{\mathbf{q}\sigma}\rangle$ with $\langle a^\dagger_{\mathbf{q}\sigma}a_{\mathbf{q}'\sigma}\rangle=(Um/2)/2E_q$ for $\mathbf{q}=\mathbf{q}'+(\pi,\pi)$ and $E_q=\sqrt{\epsilon_q^2+(Um/2)^2}$. Here, $\epsilon_q=-2t[\cos(q_x)+\cos(q_y)]$ is the usual tight-binding spectrum. Likewise, for a homogeneous superfluid d-wave state, BCS theory yields $\langle n_{\mathbf{q}}n_{\mathbf{q}'}\rangle=\langle n_{\mathbf{q}}\rangle\langle n_{\mathbf{q}'}\rangle+\Sigma_\sigma|\langle a_{\mathbf{q}\sigma}a_{\mathbf{q}'-\sigma}\rangle|^2$ with $|\langle a_{\mathbf{q}\sigma}a_{-\mathbf{q}-\sigma}\rangle|=|\Delta_q|/2E_q$, for $\mathbf{q}=-\mathbf{q}'$ and $E_q=\sqrt{(\epsilon_q-\mu)^2+\Delta_q^2}$ where $\Delta_q=2\Delta[\cos(q_x)-\cos(q_y)]$ is the d-wave gap. Pair correlations with s-wave symmetry were measured on the Bose-Einstein condensate side of a homogeneous system with a Feshbach resonance [16].

In order to examine how the antibunching dips and the pairing correlation peaks show up for the trapped lattice, we calculate $\mathcal{C}(\mathbf{q},\mathbf{q}')$ for the shell structures shown in Figs. 1 and 2. In Fig. 3 (top left), we show a 2D map of $\mathcal{C}(\mathbf{q},\mathbf{q}')$ with $\mathbf{q}'=(\pi/2,\pi/2)$ for the same parameters used in Fig. 1 (third row). Figure 3 (top right) shows a cut along the diagonal $q_x-q_x'=q_y-q_y'$. Here, in addition to the usual lattice dips [3], we clearly see the signature of the AF state in the additional antibunching dips at $q_x-q_x'=(\pm\pi,\pm\pi)$. The momentum $\mathbf{q}'=(\pi/2,\pi/2)$ is close to the Fermi surface and hence maximizes the ratio of the AF dips to the 2π lattice dips. Note that the perfect periodicity, i.e., the equal amplitude at points $\mathbf{q}\to\mathbf{q}+(n_x2\pi,n_y2\pi)$, is an artifact of the model which neglects the spatial extent of the lowest Wannier function.

We next discuss $\mathcal{C}(\mathbf{q},\mathbf{q}')$ with both AF and DSF order present, and focus on the same particle filling as above which corresponds to the second row in Fig. 2. We show in Fig. 3 (bottom left) momentum cuts in $\mathcal{C}(\mathbf{q},\mathbf{q}')$ along a diagonal line with $q_x-q_x'=q_y-q_y'$ and $\mathbf{q}'=(\pi/2,\pi/2)$ (solid line) and along a horizontal line q_x-q_x' with $q_y=0$ and $\mathbf{q}'=(\pi/2,0)$ (dashed line). Here, in addition to the AF dips, it is evident that the DSF phase displays bunching at $\mathbf{q}=-\mathbf{q}'$ since the peaks appear at $q_x-q_x'=q_x-\pi/2=-\pi$ and $\pm 2\pi$ displacements thereof. In Fig. 3 (bottom right) we fix $\mathbf{q}=-\mathbf{q}'$ and plot a 2D map of $\mathcal{C}(\mathbf{q},-\mathbf{q})$. This clearly reveals the d-wave symmetry of the pairing: the bunching is maximum along the x and y directions and minimum along $x=\pm y$. Also, the pairing is maximum around the Fermi surface as expected. The DSF pairing peaks in Fig. 3 are small and may be easier to detect at lower filling fractions where AF order is absent and a larger fraction of the particles participate in the pairing. Note that the AF antibunching dips are also present in Fig. 3 (bottom right) at $\mathbf{q}=-\mathbf{q}'=(\pm\pi/2,\pm\pi/2)$. This is an example of how the coexistence of the magnetic and superfluid order can be detected as the presence of both AF antibunching and DSF bunching peaks in expansion experiments. The AF dips disappear for lower fillings when the Fermi surface moves below $(\pm\pi/2,\pm\pi/2)$ and the density vanishes there. For the same reason there are no lattice dips at $(\pm\pi,\pm\pi)$ in this image.

In summary, we have studied the magnetic and superfluid phases of repulsive fermionic atoms on a 2D lattice combined with a harmonic trap for experimentally realistic parameters. The Hubbard correlations result in intriguing magnetic real-space shell structures which may coexist and compete with a superfluid phase. These phases show up as distinct antiferromagnetic antibunching dips and superfluid bunching peaks with d-wave symmetry in the density-density correlations which can be probed in expansion experiments. The results are relevant to current experiments on atoms in optical lattices.

B.M.A. was supported by the Danish Technical Research Council via the Framework Programme on Superconductivity.

[1] M. Greiner, O. Mandel, T. Esslinger, T. W. Hänsch, and I. Bloch, Nature (London) **415**, 39 (2002).
[2] M. Köhl, H. Moritz, T. Stöferle, K. Günter, and T. Esslinger, Phys. Rev. Lett. **94**, 080403 (2005).
[3] S. Fölling, F. Gerbier, A. Widera, O. Mandel, T. Gericke, and I. Bloch, Nature (London) **434**, 481 (2005); T. Rom, Th. Best, D. van Oosten, U. Schneider, S. Fölling, B. Paredes, and I. Bloch, *ibid.* **444**, 733 (2006).
[4] J. K. Chin, D. E. Miller, Y. Liu, C. Stan, W. Setiawan, C. Sanner, K. Xu, and W. Ketterle, Nature (London) **443**, 961 (2006).
[5] S. A. Kivelson, I. P. Bindloss, E. Fradkin, V. Oganesyan, J. M. Tranquada, A. Kapitulnik, and C. Howald, Rev. Mod. Phys. **75**, 1201 (2003).
[6] J. M. Tranquada, B. J. Sternlieb, J. D. Axe, Y. Nakamura, and S. Uchida, Nature (London) **375**, 561 (1995).
[7] T. Hanaguri, C. Lupien, Y. Kohsaka, D.-H. Lee, M. Azuma, M. Takano, H. Takagi, and J. C. Davis, Nature (London) **430**, 1001 (2004).
[8] M. Rigol, A. Muramatsu, G. G. Batrouni, and R. T. Scalettar, Phys. Rev. Lett. **91**, 130403 (2003); M. Rigol and A. Muramatsu, Phys. Rev. A **69**, 053612 (2004).
[9] S. Fölling, A. Widera, T. Müller, F. Gerbier, and I. Bloch, Phys. Rev. Lett. **97**, 060403 (2006).
[10] D. Jaksch, C. Bruder, J. I. Cirac, C. W. Gardiner, and P. Zoller, Phys. Rev. Lett. **81**, 3108 (1998).
[11] W. Hofstetter, J. I. Cirac, P. Zoller, E. Demler, and M. D. Lukin, Phys. Rev. Lett. **89**, 220407 (2002).
[12] W. Zwerger, J. Opt. B: Quantum Semiclassical Opt. **5**, S9 (2003).
[13] S. Sorella, G. B. Martins, F. Becca, C. Gazza, L. Capriotti, A. Parola, and E. Dagotto, Phys. Rev. Lett. **88**, 117002 (2002); D. Sénéchal, P.-L. Lavertu, M.-A. Marois, and A.-M. S. Tremblay, *ibid.* **94**, 156404 (2005); T. A. Maier, M. Jarrell, T. C. Schulthess, P. R. C. Kent, and J. B. White, *ibid.* **95**, 237001 (2005).
[14] I. Martin, G. Ortiz, A. V. Balatsky, and A. R. Bishop, Int. J. Mod. Phys. B **14**, 3567 (2000); M. Ichioka, M. Takigawa, and K. Machida, J. Phys. Soc. Jpn. **70**, 33 (2001); Y. Chen, Z. D. Wang, J.-X. Zhu, and C. S. Ting, Phys. Rev. Lett. **89**, 217001 (2002); B. M. Andersen and P. Hedegård, *ibid.* **95**, 037002 (2005); B. M. Andersen, I. V. Bobkova, P. J. Hirschfeld, and Yu. S. Barash, Phys. Rev. B **72**, 184510 (2005); B. M. Andersen, P. J. Hirschfeld, A. P. Kampf, and M. Schmid, Phys. Rev. Lett. **99**, 147002 (2007).
[15] E. Altman, E. Demler, and M. D. Lukin, Phys. Rev. A **70**, 013603 (2004).
[16] M. Greiner, C. A. Regal, J. T. Stewart, and D. S. Jin, Phys. Rev. Lett. **94**, 110401 (2005); G. D. Gu, G. Xu, M. Fujita, and K. Yamada, Nature (London) **429**, 534 (2004).